1970

Auger Electrons from Argon with Energies 150-210 eV Produced by H^+ and H_2 Impacts

D. J. Volz
Georgia Institute of Technology, Atlanta, Ga.

M. Eugene Rudd
University of Nebraska - Lincoln, erudd@unl.edu

Auger Electrons from Argon with Energies 150-210 eV Produced by H^+ and H_2^+ Impacts

D. J. Volz * and M. E. Rudd

Behlen Laboratory of Physics, University of Nebraska, Lincoln, Nebraska 68508

Received 27 April 1970

Secondary electrons in the energy range 150-210 eV produced by 125-300-keV H^+ and H_2^+ impacts on argon gas are measured as a function of their energy and angle of emission. Discrete line spectra are due to Auger transitions from L_2 and L_3 vacancy states as well as satellite transitions from multivacancy states. The widths, energies, and branching ratios of the L_2 and L_3 vacancy states are presented. Widths of these states are appreciably greater than those obtained with electron impact excitation. This can be attributed to the recoil velocities of the target atom and to the presence of the proton in the vicinity of the emitting atom. The angular distribution of Auger electrons is found to be nearly isotropic, in marked contrast to electrons in the continum spectrum. The cross sections for the production of $L_{2,3}$ and L_3 vacancy states are determined as a function of impact energy.

Published in *Physical Review A* 2, 1395 - 1403 (1970)

URL: http://link.aps.org/doi/10.1103/PhysRevA.2.1395
DOI: 10.1103/PhysRevA.2.1395

* Present address: Georgia Institute of Technology, Atlanta, Ga.

PHYSICAL REVIEW A VOLUME 2, NUMBER 4 OCTOBER 1970

Auger Electrons from Argon with Energies 150–210 eV Produced by H^+ and H_2^+ Impacts*

D. J. Volz† and M. E. Rudd
Behlen Laboratory of Physics, University of Nebraska, Lincoln, Nebraska 68508
(Received 27 April 1970)

Secondary electrons in the energy range 150–210 eV produced by 125–300-keV H^+ and H_2^+ impacts on argon gas are measured as a function of their energy and angle of emission. Discrete line spectra are due to Auger transitions from L_2 and L_3 vacancy states as well as satellite transitions from multivacancy states. The widths, energies, and branching ratios of the L_2 and L_3 vacancy states are presented. Widths of these states are appreciably greater than those obtained with electron impact excitation. This can be attributed to the recoil velocities of the target atom and to the presence of the proton in the vicinity of the emitting atom. The angular distribution of Auger electrons is found to be nearly isotropic, in marked contrast to electrons in the continum spectrum. The cross sections for the production of $L_{2,3}$ and L_3 vacancy states are determined as a function of impact energy.

I. INTRODUCTION

When electrons emitted from photon-, electron-, or ion-atom collisions are energy-analyzed with sufficient resolution, structure appears in the spectrum which results from autoionization or Auger transitions in the atom. Earlier work at this laboratory[1] has shown that two of the electron energy regions of interest in argon are 0–15 and 150–210 eV. The low-energy fine structure is associated with excitations of M-shell electrons, while the higher-energy peaks are Auger transitions from single L-shell vacancy states and satellite lines from simultaneous L- and M-shell vacancies.

Using electron impact excitation, Mehlhorn[2] and Mehlhorn and Stahlherm[3] have studied Auger transitions from L_1, and L_2, and L_3 vacancies in argon. Nakamura *et al.*[4] have investigated structure near the L_2 and L_3 edges in argon by absorption of synchrotron light and obtain values for the energies of these edges. Deslattes[5] has deduced new values of the L_2 and L_3 levels from K-series x-ray measurements. Ogurtsov and co-workers[6,7] have studies the production of vacancy states in argon using H^+, Ne^+, and Ar^+ beams up to 20 keV. Cacak[8] has made cross-section measurements at low resolution of the production of argon vacancy states by Ar^+ beams from 50 to 300 keV.

This paper reports on fairly high-resolution measurements of energies and intensities of Auger and satellite lines in the 150–210 eV region of the

argon spectrum excited by collisions of H^+ and H_2^+ ions of 125–300-keV energy. The angular distribution of electrons from four transitions is measured, branching ratios from initial single vacancy states are given, widths of the lines corrected for analyzer broadening are determined, and absolute values of excitation cross sections are presented.

II. EXPERIMENTAL ARRANGEMENT

The apparatus is similar to that described previously.[9,10] Ion beams of 125–300-keV energy are magnetically analyzed before entering the collision chamber. The energy drift during a typical run is less than 1 keV. The chamber is equipped with ports at nine angles between 10 and 160°, to any one of which a parallel-plate electrostatic analyzer may be attached. Three pairs of mutually perpendicular 120-cm-diam Helmholtz coils are used to compensate for the earth's magnetic field and stray 60-Hz fields in the collision region.

The pressure of the target gas, measured by a Baratron capacitance manometer, is between 1.2 and 1.6 mTorr. Data of Normand[11] are used to correct for the absorption of electrons between the collision region and the detector. The transmission t is about 80% at the pressures used.

Individual electrons are detected by a Dumont electron multiplier with copper-beryllium dynodes. Pulses are amplified and converted to a dc voltage proportional to count rate. This voltage is divided by a voltage proportional to the primary ion beam current. The resulting ratio is continuously plotted on the y axis of a recorder, while the x axis displays the electron energy. The parallel-plate analyzer is operated with a constant voltage between the plates while the back plate voltage is varied. This mode of operation ensures a constant resolution as the spectrum is scanned. The resolution is varied by changing the front-to-back plate voltage. In the work reported here the full widths at half-maximum (FWHM) of the transmission function of the analyzer are 0.9 and 0.22 eV.

III. DATA ANALYSIS

The primary quantity measured in this experiment is the doubly differential cross section $\sigma(E, \theta)$, where E is the ejected electron energy and θ is the angle between the primary ion beam and the path of the electron. The number of electrons per second at the detector is

$$n_e = I_0 n \Delta x \Delta \Omega \int f(E, E_0)\, \sigma(E, \theta)\, t\, dE, \qquad (1)$$

where I_0 represents the number of incident ions per second, n is the density of target atoms, Δx is the length of beam viewed by the analyzer, $\Delta\Omega$ is the mean solid angle subtended at the scattering center by the analyzer entrance slit, and t is the transmission of the target gas for electrons. The transmission function of the analyzer is $f(E, E_0)$, where E_0 is the mean energy the analyzer is set to accept. The integral in (1) is over the transmission function of the analyzer. This equation assumes that $\sigma(E, \theta)$ does not vary appreciably over the range of angles accepted by the defining slits. The approximate angular range for the analyzer used is $\pm 1.2°$.

On the basis of a simple theory of electrostatic analyzers which neglects the angular aberration terms, the transmission function is trapezoidal in shape with the base width proportional to the sum of the widths of the entrance and exit slits and a top width proportional to the difference of the widths of the same slits. The parameters of the transmission function are determined by the use of an electron gun mounted to simulate electrons emitted from the collision region.

The experimental arrangement is such that the ordinate of the graph from the recorder is proportional to the ratio n_e / I_0. Using the result quoted by Kuyatt[12] for $\Delta x \Delta \Omega$, and substituting for n from the ideal-gas law, we obtain the following expression for the ordinate:

$$y(E_0) \propto \frac{Pt}{T \sin\theta} \int f(E, E_0)\, \sigma(E, \theta)\, dE\ , \qquad (2)$$

where P is the gas pressure and T its temperature. We ignore the small dependence of t on electron energy over the range investigated. We also omit factors correcting for the focusing of the electron beam prior to entering the analyzer and the efficiency of the electron detector. Neither of these effects is found to be important.

It is necessary to determine the constant of proportionality in (2) in order to obtain values of $\sigma(E, \theta)$. This is done by comparison with absolute cross-section measurements in the continuum made under lower resolution in this laboratory.[13] The comparison is made over a wide range of primary ion energies and angles of ejection for electrons of 150-eV energy. Determined in this way, the uncertainty in our absolute values of cross sections is ±50%.

We assume that the cross section representing an Auger transition from state i to state j is of the Breit-Wigner form[14]

$$\sigma(E, \theta, \Gamma_i) = \frac{\Gamma_i}{2\pi} \frac{I_{ij}(\theta)}{(E - W_{ij})^2 + \frac{1}{4}\Gamma_i^2}\ , \qquad (3)$$

where Γ_i is the FWHM and W_{ij} is the mean energy of the transition. The normalization is such that $I_{ij}(\theta)$ is the cross section for the transition differential in angle only.

To find the linewidth Γ_i it is necessary to account

for the effect of the analyzer resolution since it contributes a comparable width. This is done as follows. Define the convolution $S(E_0 - W_{ij}, \Gamma_i)$ of the Breit-Wigner line shape with the analyzer transmission function by the equation

$$I_{ij}(\theta) S(E_0 - W_{ij}, \Gamma_i) = \int f(E, E_0)\, \sigma(E, \theta, \Gamma_i)\, dE \,. \quad (4)$$

The integration is performed analytically to obtain the function S. With the measured parameters of the analyzer transmission function and a proper choice of the linewidth, the calculated function S very closely approximates the measured line shapes. A plot of the FWHM of the function S versus Γ_i is used in determining actual linewidths from the measured widths.

If Eq. (4) is now integrated over E_0, we have on the right-hand side just the area under a peak of the experimental curve which is shown by Kuyatt[12] to reduce to the product of $I_{ij}(\theta)$ and the area under the transmission function of the analyzer. This implies that for any analyzer the integral of S over E_0 equals the area under the transmission function of the analyzer. We have shown for our specific function that this is true. This enables us to determine the differential cross section $I_{ij}(\theta)$ for a given transition either from a measurement of the area under the corresponding peak on the graph or by fitting $S(E_0 - W_{ij}, \Gamma_i)$ to the shape of the peak. Having determined $I_{ij}(\theta)$ as a function of angle we can integrate over all angles to obtain the cross section I_{ij} which is the emission cross section for a given transition. In addition, if we sum the cross sections of all possible autoionizing transitions from an initial state i we obtain the cross section I_i for depopulation of this state via autoionization. The quantity I_i is equal to the excitation cross section of state provided two conditions are met. One is that the level i is not populated by radiative or nonradiative transitions from a higher level, and the second is that the only mode of depopulation of level i is through autoionization. In the work reported here the first condition would imply the absence of autoionizing transitions from higher levels. Such transitions are not observed in our work. The second condition is met to a very good approximation since the L fluorescence yield for argon is very small, probably less than 1%.[15]

IV. RESULTS AND DISCUSSION

A. Identification of Transitions

The spectrum of secondary electrons has the usual continuum, probably owing to direct Coulomb ionization, and peaks or lines due to both Auger and satellite transitions. To facilitate subtraction of the continuum, runs were made into the continuum at both ends of the fine-structure region and a smooth curve constructed by extrapolation.

To verify previous identifications[1,3] of transitions from L_2 and L_3 states which were made primarily by comparing the energy differences of the experimental lines with known differences of possible final states, a technique is employed which may prove of general usefulness. This method makes use of the fact that certain classes of states are relatively more strongly excited by ions of one type than by those of another. We use both H^+ and H_2^+ ions for this method of identification. The spectra at moderate resolution are shown in Figs. 1 and 2. The peaks are numbered arbitrarily for identification.

We define a ratio

$$R_{ijkl} = I_{ik}(\theta)/I_{jl}(\theta)$$

relating the intensities of two transitions as produced by a particular ion. By choosing a given line to represent the j to l transition, R_{ijkl} can be calculated for all lines with respect to this "standard." The quantity

$$R = R_{ijkl}(H^+) - R_{ijkl}(H_2^+)$$

is then examined to group the transitions. The ratio difference R equals zero if the two transitions are from the same initial level, i.e., $i=j$, or if the two transitions are from different levels which are excited in the same ratio by H^+ and H_2^+. Conversely if $R \neq 0$ the transitions are from different levels and one of these states is relatively more strongly excited by one of the ions.

The histograms of Fig. 3 show the ratio difference R plotted for various lines using both an Auger line (No. 25) and a satellite line (No. 22) for the standard. All previously identified Auger lines from $L_{2,3}$ vacancy states (Nos. 9, 11, 15–17, 19, 24–26, and 27) except No. 19 have R values within 0.05 of zero in Fig. 3(b) in conformity with the above discussion. The line No. 19 is an unresolved combination of an Auger and a satellite transition. It is doubtful that L_2 transitions can be separated from L_3 transitions with this technique since within the accuracy of our data these levels are excited in the same ratio by H^+ and H_2^+. The above discussion can be applied to the satellite lines Nos. 12, 18, 20–22, and 23. Further identification of these satellite lines cannot be made until the resolution is improved.

In some cases the same projectile at two different energies will excite levels differently, in which case this method may also be used.

B. Calibration of Energy Scale

The energy in eV of electrons passed by the parallel-plate analyzer is related[9] to the front and

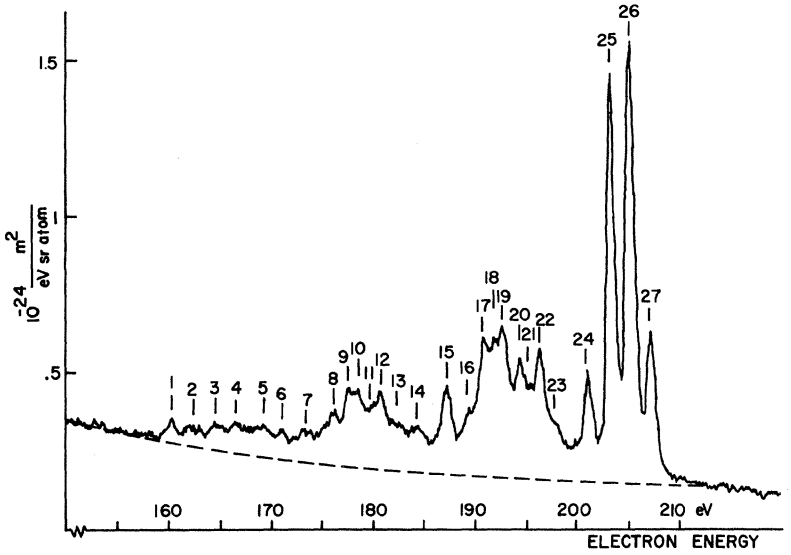

FIG. 1. Spectrum of electrons at 130° from 300-keV H^+-Ar collisions. The analyzer resolution was 0.9 eV. The dashed line representing the continuum is estimated by extrapolation from the continuum at both ends. The peaks are numbered arbitrarily for identification.

back plate potentials (V_s and V_a, respectively) by the equation

$$E = V_a/c + (c-1)\,V_s/c\,,$$

where c is the constant of the analyzer. If the potential difference $V_f = V_a - V_s$ is held constant, then the relation reduces to $E = V_a + \text{const}$, and the scale factor has disappeared. Then calibration of the energy scale requires only a single known energy line. For this we have taken the energy of L_3 to be 248.43 ± 0.05 eV as given by Deslattes,[5] and the $M^2_{2,3}(^1S)$ state to be at 47.51 eV from the compilation by Moore[16] thus giving 200.92 eV for the energy of peak No. 24. This is chosen as the standard since it is a singlet with no interfering satellite transitions. From this standard all other peak energies are measured and the results are given in Tables I and II. The higher-resolution spectra from which these measurements are taken are shown in Figs. 4 and 5.

The calculated energies in Table I are obtained by assuming the energies of the L_3 and L_2 states as 248.43 and 250.60 eV, respectively, and using the final-state energies from Moore[16] for all except the state $M^2_1(^1S)$. Since this is not available spectroscopically we use the value 70.61 eV as determined by Mehlhorn.[3] The lines Nos. 17, 19, 26, and 27 all involve a triplet final state. Since we do not resolve the triplet structure the calculated energies are a weighted average. The weighting factors, which were different for the two different initial states, are taken from Mehlhorn.[3]

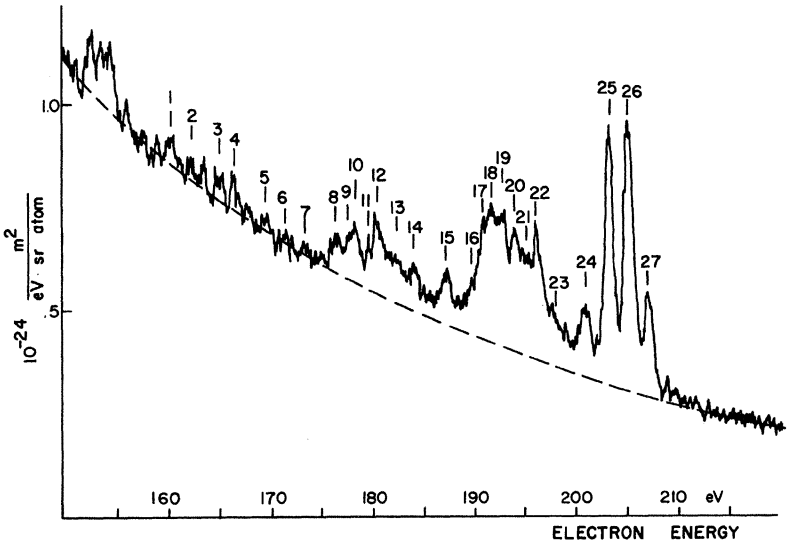

FIG. 2. Spectrum of electrons at 130° from 300-keV H_2^+-Ar collisions. Resolution was 0.9 eV.

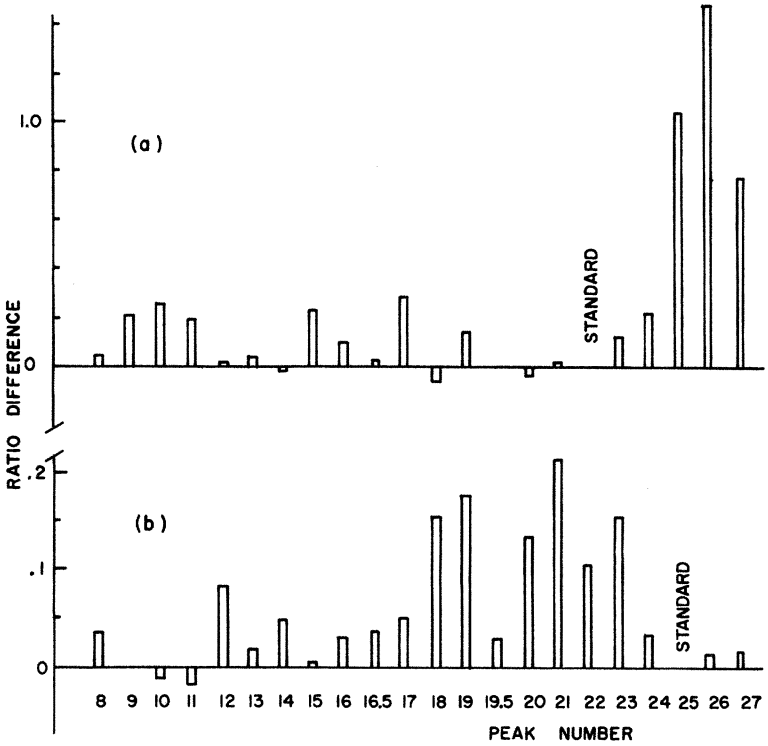

FIG. 3. Histogram used to group transitions arising from same initial state. Peaks which have small or zero ratio differences originate from the same state as the standard or are excited in the same ratio. (a) Standard is a satellite line. (b) Standard is the Auger transition L_3-$M^2_{2,3}$ (^{1}D) + e.

The agreement between our measured energies, the calculated values, and those measured by Mehlhorn is generally very good. The chief exception involves the M_1^2 (^1S) state, which by our measurements, should be at 70.72 eV, somewhat higher than Mehlhorn's value.

Our value of the L_2-L_3 spacing is 2.17 ± 0.07 eV, which compares favorably with the values 2.18 of Deslattes[5] and 2.14 ± 0.02 eV of Mehlhorn,[3] but poorly with Nakamura's value[4] of 2.03 and Lindh's[17] 2.07 eV. A definitive new measurement of the spin splitting has been made by Krause,[18]

TABLE I. Transition energies and linewidths: L-MM transitions.

Final state	Peak No.	Measured[a] energy (eV ± 0.07 eV)	Calculated[b] energy (eV)	Mehlhorn (Ref. 3) (eV ± 0.25 eV)	Linewidth (eV ± 0.05 eV)
		L_2 ($^2P_{1/2}$) Initial state			
M_1^2 (^1S)	11	179.88	179.99	179.93	0.35
$M_1M_{2,3}$ (^1P)	16	189.35	189.36	189.30	0.33
(^3P)	19	192.93	192.96	192.88	···
$M_{2,3}^2$ (^1S)	24.9	203.03	203.09	203.01	···
(^1D)	26.5	205.46	205.48	205.40	0.25
(^3P)	27	207.16	207.10	207.03	0.26
		L_3 ($^2P_{3/2}$) Initial state			
M_1^2 (^1S)	9	177.68	177.82	177.79	0.25
$M_1M_{2,3}$ (^1P)	15	187.13	187.19	187.16	0.24
(^3P)	17	190.98	190.91	190.88	0.40
$M_{2,3}^2$ (^1S)	24	200.92	200.92	200.87	0.24
(^1D)	25	203.31	203.31	203.26	0.24
(^3P)	26	205.05	205.00	204.96	0.33

[a]Peak No. 24 was taken as the standard with an energy of 200.92 eV.

[b]Calculated using the values 248.43 and 250.60 eV for the L_3 and L_2 states and using final-state energies determined from Ref. 16 except the value 70.61 eV was taken from Ref. 3 for the M_1^2 (^1S) state.

TABLE II. Transition energies and relative intensities: satellite lines.

Peak No.	Measured energy (eV ± 0.07 eV)	Relative intensity[a] (No. 24 = 100)
1	160.39	18
2	162.61	14
3	164.68	19
4	166.45	23
5	169.75	23
6	171.42	21
7	173.33	35
7.5	175.32	14
7.6	175.72	20
8	176.29	44
9.6	178.31	14
10	178.72	55
10.5	179.22	17
12	180.70	90
12.5	181.83	30
13	182.94	26
14	184.22	44
16.5	190.31	40
18	192.08	96
18.5	192.48	4
18.9	192.76	87
19.5	193.79	23
19.6	194.05	8
20	194.47	140
21	195.38	77
22	196.41	120
22.5	197.33	23
23	197.97	37

[a]Relative intensities of peaks Nos. 1–6 are measured with 300-keV H^+ impacts. The rest are measured with 275-keV H^+ impacts. The uncertainties of 1–6 are ± 20% while the rest are ± 10%.

who used a spherical electrostatic analyzer to produce an Auger spectrum of electrons from argon excited by 3.97-keV electron impact. His value is 2.163 ± 0.011 eV.

C. Cross Sections and Branching Ratios

The summation of emission cross sections for various transitions from a given initial state is done by a combination of the two methods described in Sec. III. The area under a pair of unresolved peaks could be measured (with a planimeter) to yield the sum of the cross sections for two transitions more accurately than either transition could be determined separately. For this reason the sum of the L_2 and L_3 excitation cross sections is more accurate than the excitation cross section determined for each level. To obtain cross sections for individual transitions in regions where n different transitions contributed intensity to the spectrum, an $n \times n$ matrix is solved, each element of which was the convolution of the Breit-Wigner line shape and the analyzer transmission function. The solution yields the values $I_{ij}(\theta)$ for each transition. From these results the branching ratios are obtained and are listed in Table III. The agreement with Mehlhorn's values is only fair. Our spectra are somewhat noisier than his and, furthermore, since ion collisions produce double vacancy states more strongly than electrons,[19] in some cases an interfering satellite transition causes a greater error in our work than in the electron work.

The ratio of L_3 to L_2 level cross sections should be equal to the ratio of the $2j+1$ values for the levels and, within our experimental uncertainty, this is found to be so.

Table IV gives a comparison between the excitation of various levels by protons and by H_2^+ ions of the same velocity or of the same energy. From simple considerations it may be expected that the ratio of excitation by 300-keV H_2^+ to that by 150-keV H^+ should be unity. Although this is almost

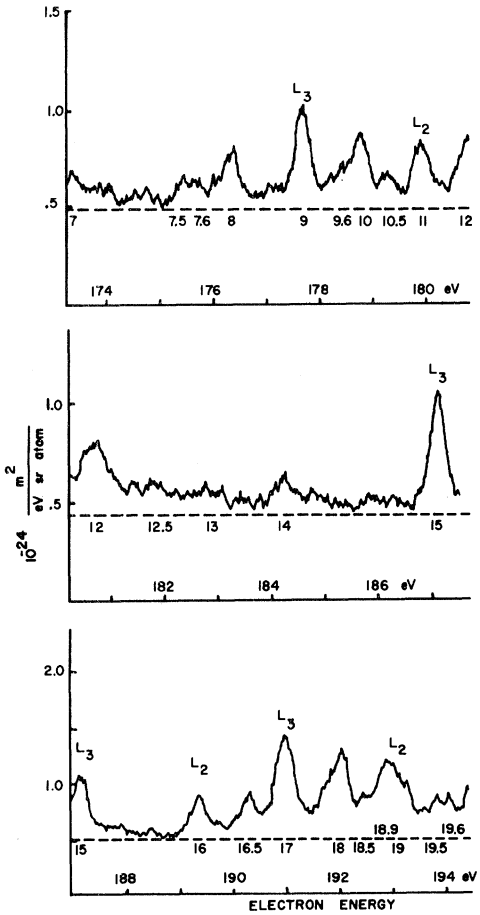

FIG. 4. High-resolution spectrum at 160° for 275-keV H^+-Ar collisions. The Auger transitions are labeled by their initial vacancy states. Resolution 0.22 eV.

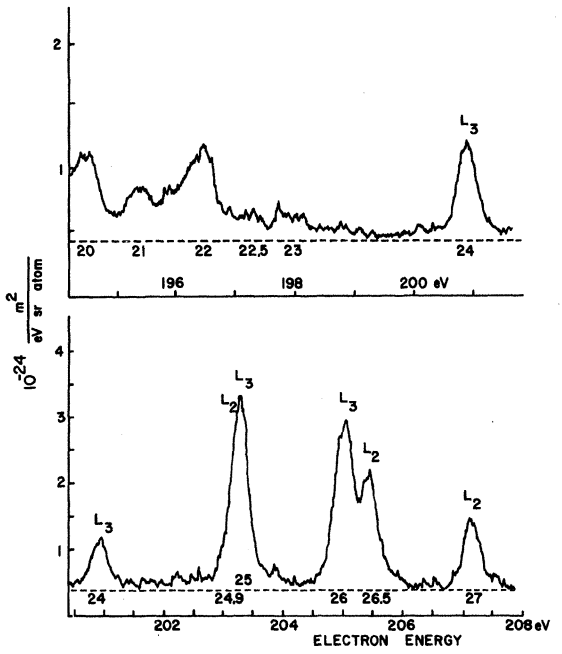

FIG. 5. High-resolution spectrum at 160° for 275-keV H^+-Ar collisions. Resolution 0.22 eV.

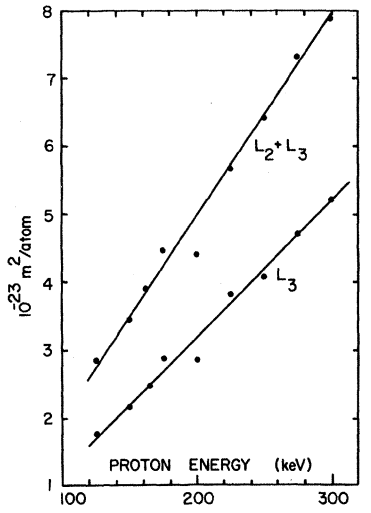

FIG. 6. Cross section for the production of single vacancy states versus proton impact energy. Upper curve is for the sum of the cross sections for producing L_2 and L_3 vacancies.

true for the L_2 and L_3 states, it is not for the multivacancy states. The factor of 2 difference in the population of the single and multiple vacancy states created by 300-keV projectiles of the two types is the prerequisite for the effectiveness of the identification procedure described in Sec. II.

Figure 6 shows the variation with proton energy of the cross section for producing L_3 vacancies and the sum of the cross sections for producing L_2 and L_3 vacancies. For both there is an approximately linear increase with energy. There are at least two processes which could produce the observed vacancies: ionization and asymmetrical charge transfer. Two theoretical methods of calculating the ionization cross section[20,21] give cross sections higher than our data. Calculations of the charge transfer give both higher[22] and lower values.[23] Further work needs to be done on the theory of the production of vacancy states in the range of ion velocities comparable to the electron velocities in the shell under study.

D. Angular Distributions

Runs made at all nine angles from 10 to 160° for 300-keV protons on argon determine the emission cross section as a function of angle for four of the Auger transitions. These are shown in Fig. 7. The error bars represent the reproducibility of the data taken at the two opposing 90° ports. The four transitions appear to be essentially isotropic, with only slight variations with angle apparent. Although these variations are mostly within experimental uncertainties, an attempt is made to fit the curve for line No.25 with a series of spherical harmonics. A least-squares fit yields the equation

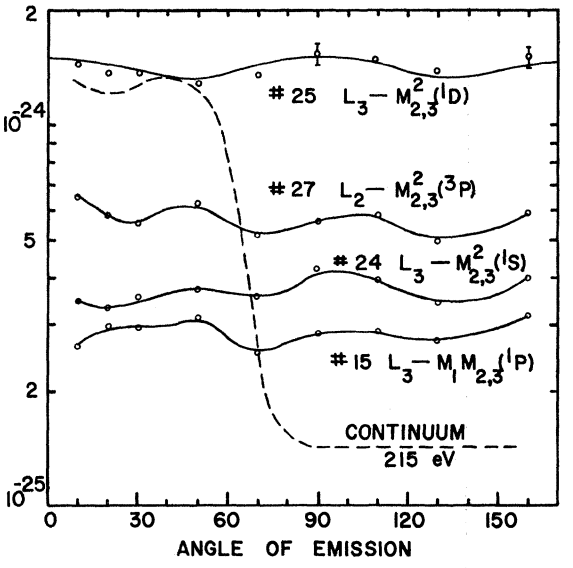

FIG. 7. Angular distribution of electrons from 300-keV H^+-Ar collisions for four Auger transitions and for continuum electrons at 215 eV. The distribution for peak No. 25 is fitted by a series of spherical harmonics (see text). The units of the ordinate are m^2/sr for the Auger transitions and represents areas integrated under the peaks. The units are $m^2/eV\ sr$ for the continuum cross sections.

TABLE III. Branching ratios for L-MM Auger transitions.

Final state	L_2-MM Present expt	Mehlhorn expt (Ref. 3)	L_3-MM Present expt	Mehlhorn expt (Ref. 3)	Mehlhorn expt (Ref. 3)
M_1^2 (^1S)	0.086 ± 0.02	0.055 ± 0.005	0.066 ± 0.009	0.057 ± 0.005	0.023
$M_1M_{2,3}$ (^1P)	0.089 ± 0.02	0.065 ± 0.002	0.075 ± 0.01	0.063 ± 0.002	0.124
(^3P)	0.145 ± 0.03	0.103 ± 0.006	0.147 ± 0.02	0.088 ± 0.002	0.124
$M_{2,3}^2$ (^1S)	0.05 ± 0.02	0.096 ± 0.005	0.095 ± 0.01	0.097 ± 0.002	0.059
(^1D)	0.42 ± 0.09	0.373 ± 0.008	0.35 ± 0.05	0.364 ± 0.006	0.363
(^3P)	0.25 ± 0.05	0.308 ± 0.006	0.27 ± 0.03	0.331 ± 0.008	0.306

$$I_{ij}(\theta) = 14.16 - 1.23\ Y_{20} + 1.87\ Y_{40}$$

in units of 10^{-24} m^2/sr. A plot of this equation is shown for line No. 25 in Fig. 7. The fit is slightly better than for a straight line. For comparison the cross section for producing electrons in the continuum at 215 eV is shown. By contrast a strong angular dependence is evident with relatively few electrons of that energy found at angles above 90°.

E. Linewidths

The method described in Sec. III is used to determine the widths of lines originating from the L_2 and L_3 states from the measured widths for the various transitions from these states. The results are given in Table I. Widths measured in this way vary from 0.24 to 0.40 eV, values considerably above the 0.16 ± 0.02 eV of Mehlhorn[3,24] and Rubinstein's theoretical value[25] of 0.10 eV. The agreement is better with the value 0.25 ± 0.1 eV given by Deslattes[26] but his value represents an upper limit. In some cases (notably peaks Nos. 17 and 19) it is possible that there are nearby unresolved satellite lines adding to the apparent widths. After eliminating such lines we obtain an average of 0.28 eV.

There are at least two effects which contribute significantly to the difference between our widths using ion impact excitation and those of Mehlhorn, who used electron impacts. One is a Doppler broadening[27,1] caused by a distribution of directions of the recoil velocities. Assuming a 300-keV impact with a distance of closest approach of 0.1 Å, the recoil energy calculated using a screened Coulomb potential is about 0.24 eV and the corresponding Doppler spread viewed from 160° is about 0.036 eV. The recoil from an electron impact, on the other hand, is negligible.

Another effect on the linewidth comes from the presence of the projectile ion near the atom at the time the Auger electron is emitted. If the mean lifetime of an Auger state is 4×10^{-15} sec, a 300-keV proton is, on the average, about 300 Å away at the moment of emission. The potential at that distance from a proton is raised by about 0.05 V. Barker and Berry[28] have worked out the theory of the broadening by this mechanism, and using their results we find this contributes about 0.054 eV to the width. Since the velocity of Mehlhorn's 2-keV electrons is about 3.5 times as great as our 300-keV protons, this effect would be proportionately smaller in his case.

TABLE IV. Relative excitation of vacancy states by H^+ and H_2^+.

Vacancy state	$\frac{I(300\text{-keV } H_2^+)}{I(300\text{-keV } H^+)}$	$\frac{I(300\text{-keV } H_2^+)}{I(150\text{-keV } H^+)}$
L_2	1.24 ± 0.19	0.50 ± 0.11
L_3	1.18 ± 0.19	0.52 ± 0.13
$\sum_i LM^i$	1.49 ± 0.15	0.91 ± 0.13

ACKNOWLEDGMENTS

We wish to express our thanks to Dr. W. Mehlhorn for informative and helpful discussions, and to Dr. M. Krause for permission to use his unpublished data.

*Research supported by the National Science Foundation and performed in partial fulfillment of requirements for the Ph. D. degree at the University of Nebraska.

†Present address: Georgia Institute of Technology, Atlanta, Ga.

[1]M. E. Rudd, T. Jorgensen, Jr., and D. J. Volz, Phys. Rev. 151, 28 (1966).

[2]W. Mehlhorn, Z. Physik 208, 1 (1968).

[3]W. Mehlhorn and D. Stalherm, Z. Physik 217, 294 (1968).

[4]M. Nakamura, M. Sasanuma, S. Sato, M. Watanabe, H. Yamashita, Y. Iguchi, A. Ejiri, S. Nakai, S. Jamaguchi, T. Sagawa, Y. Nakai, and T. Oshio, Phys. Rev. Letters 21, 1303 (1968).

[5]R. D. Deslattes, Phys. Rev. 186, 1 (1969).

[6]G. N. Ogurtsov, I. P. Flaks, S. V. Avakyan, and N. V. Fedorenko, Zh. Eksperim. i Teor. Fiz. Pis'ma v Redaktsiyu 8, 541 (1968) [Soviet Phys. JETP Letters 8, 330 (1968)].

[7]G. N. Ogurtsov, I. P. Flaks, and S. V. Avakyan, in

Proceedings of the Sixth International Conference on the Physics of Electronic and Atomic Collisions, abstracts of papers (MIT Press, Cambridge, Mass., 1969), p. 274.

[8]R. K. Cacak and T. Jorgensen, Jr. Phys. Rev. A 2, 1322 (1970).

[9]M. E. Rudd, Rev. Sci. Instr. 37, 971 (1966).

[10]M. E. Rudd and T. Jorgensen, Jr., Phys. Rev. 131, 666 (1963).

[11]C. E. Normand, Phys. Rev. 35, 1217 (1930).

[12]C. E. Kuyatt, in *Methods of Experimental Physics*, Vol. 7a, edited by L. Marton (Academic, New York, 1968), p. 1.

[13]J. B. Crooks and M. E. Rudd (unpublished).

[14]J. M. Blatt and V. F. Weisskopf, *Theoretical Nuclear Physics*, (Wiley, New York, 1952), p. 412.

[15]A. W. Fink, R. C. Jopson, H. Mark, and C. D. Swift, Rev. Mod. Phys. 38, 536 (1966).

[16]C. E. Moore, *Atomic Energy Levels*, Natl. Bur. Std. Circular No. 467 (U.S. GPO, Washington, D.C. 1949), Vol. I.

[17]A. E. Lindh and A. Nilsson, Arkiv Mat. Astron. Fys. 31A, No. 7 (1945); 31B, No. 11 (1945).

[18]Manfred O. Krause (private communication).

[19]A. K. Edwards and M. E. Rudd, Phys. Rev. 170, 140 (1968).

[20]L. Vriens, Proc. Phys. Soc. 90, 935 (1967). See also J. D. Garcia, Phys. Rev. A 1, 280 (1970).

[21]E. Merzbacher and H. W. Lewis, *Encyclopedia of Physics*, (Springer, Berlin, 1958), Vol. 34, p. 166.

[22]D. Rapp and W. E. Francis, J. Chem. Phys. 37, 2631 (1962).

[23]D. R. Bates and R. A. Mapleton, Proc. Phys. Soc. 90, 909 (1967).

[24]W. Mehlhorn, D. Stalherm, and H. Verbeek, Z. Naturforsch. 23a, 287 (1968).

[25]R. A. Rubinstein, Ph.D. Thesis, University of Illinois, 1955 (unpublished).

[26]R. D. Deslattes, Phys. Rev. 133, A390 (1964).

[27]M. E. Rudd, T. Jorgensen, Jr., and D. J. Volz, Phys. Rev. Letters 16, 929 (1966).

[28]R. B. Barker and H. W. Berry, Phys. Rev. 151, 14 (1966).